

TAEPPo: Topology-Aware Relational Attention Networks with Adaptive-Entropy Proximal Policy Optimization for Flexible Job Shop Scheduling

Anonymous Authors

Abstract

The Flexible Job-Shop Scheduling Problem (FJSP) is a cornerstone optimization challenge in smart manufacturing, requiring the simultaneous assignment of precedence-constrained operations to eligible machines. Given its NP-hard complexity, deep reinforcement learning (DRL) has emerged as a potent paradigm for deriving real-time scheduling policies with advanced scalability and robust generalization. However, existing DRL-based scheduling methods often face two critical limitations: the insufficient extraction of multi-granular topological relations and the inherent instability of algorithmic adaptation. To overcome these, we propose TAEPPo, a novel framework that integrates Topology-Aware Relational Attention Networks (TARAN) with Adaptive-Entropy Proximal Policy Optimization (AEPPo). Specifically, TARAN decomposes the scheduling graph into dual relational attention networks: one encodes operation embeddings by synthesizing local operation-level adjacency with global job-level context, while the other characterizes machine embeddings through heterogeneous operation-machine relations. Furthermore, AEPPo stabilizes the training trajectory via automated entropy regularization, dynamically balancing the exploration-exploitation trade-off across discrete decision-making spaces. Extensive experiments demonstrate that TAEPPo consistently outperforms both traditional PDRs and state-of-the-art DRL-based methods on diverse benchmarks, significantly improving feature representation extraction and policy optimization robustness.

1 Introduction

In the drive toward Industry 4.0 technologies [Xu *et al.*, 2021; Ahmed *et al.*, 2022], optimizing resource allocation and production sequencing is a paramount challenge to achieve operational excellence in modern manufacturing systems [Ahmed and Siddique, 2022; Mahmoodi *et al.*, 2024]. Within this domain, the Flexible Job-Shop Scheduling Problem (FJSP) is recognized as a central and critical NP-hard combinatorial optimization problem [Xie *et al.*, 2019; Dauzère-Pérès *et al.*,

2024], defined by the management of a finite set of jobs and machines. Each job consists of an ordered collection of operations governed by inherent precedence constraints, with each operation needing to be assigned to one of several compatible machines [Lei *et al.*, 2022]. The objective of this complex problem is typically to maximize throughput efficiency by minimizing the makespan, which refers to the maximum completion time [Chaudhry and Khan, 2016].

Recently, deep reinforcement learning (DRL) has been widely adopted to address FJSP [Han and Yang, 2021; Liu *et al.*, 2022; Yuan *et al.*, 2024; Wang *et al.*, 2025], outperforming traditional exact methods [Meng *et al.*, 2020], metaheuristics [Gao *et al.*, 2019], and heuristic priority dispatch rules (PDRs) [Demir and Yilmaz, 2021] in terms of both computational efficiency and scheduling quality. DRL-based scheduling methodologies model the decision-making process as a Markov Decision Process (MDP) [Lei *et al.*, 2023], providing an end-to-end learning framework [Wang *et al.*, 2021] to define states, actions, state transitions and rewards. This formulation enables agents to autonomously learn and optimize dynamic PDRs through iterative environment interactions.

The intricate nature of FJSP, compounded by stringent intra-job precedence constraints and machine assignment flexibility, demands robust structural representations to navigate the complex solution space [Smit *et al.*, 2025]. Consequently, there is a growing trend towards integrating specialized graph neural networks (GNNs) [Zhou *et al.*, 2020; Corso *et al.*, 2024] into DRL architectures to encode high-dimensional correlations and dynamic dependencies within the scheduling state. Specifically, recent studies have effectively utilized the disjunctive graph [Brandomarte, 1993; Zhang *et al.*, 2024] for comprehensive state representation, achieving remarkable advancements within this field [Song *et al.*, 2022; Wang *et al.*, 2023; Zhao *et al.*, 2025].

However, existing DRL-based scheduling methods exhibit two critical challenges. First, they typically treat the scheduling graph as a monolithic entity, thereby impeding the distillation of inherent multi-granular topological relations. These models predominantly restrict operation embeddings to local precedence chains [Song *et al.*, 2022; Wang *et al.*, 2023], focusing exclusively on immediate adjacency relations (predecessors and successors) while overlooking the global job-level context. However, such global semantics are critical to evaluate both scheduled and remaining workloads, enabling

the agent to optimize resource allocation across the entire production horizon. Second, most prevailing methods directly employ vanilla DRL algorithms [Yuan *et al.*, 2024; Zhao *et al.*, 2025], such as standard proximal policy optimization (PPO) [Schulman *et al.*, 2017] and deep Q-learning (DQN) [Du *et al.*, 2022], without domain-specific adaptation. These generic implementations are often ill-suited for navigating the dynamic, discrete decision-making spaces and the intricate resource bottlenecks, resulting in limited robustness and suboptimal performance.

To address the aforementioned limitations, we present an advanced framework, named TAEPPPO, which synergistically integrates topology-aware relational attention networks (TARAN) with adaptive-entropy proximal policy optimization (AEPPO). Firstly, the TARAN module is engineered to extract multi-granular structural relations by decomposing the scheduling graph into dual relational attention streams. By incorporating local operation-level adjacency and global job-level context for operation embeddings, and mapping heterogeneous operation-machine relations for machine embeddings, TARAN facilitates a multi-granular feature extraction that transcends conventional precedence chains. Secondly, AEPPO stabilizes learning trajectories through an adaptive entropy regularization to dynamically balance stochastic exploration and deterministic exploitation, thereby accelerating convergence robustness and improving policy generalization relative to the vanilla PPO algorithm. The main contributions are stated as follows:

- We propose the TARAN module, which decouples graph feature extraction to characterize operation embeddings by incorporating local operation-level adjacency and global job-level context relations, while simultaneously deriving machine embeddings by encoding heterogeneous operation-machine relations.
- We develop the AEPPO algorithm, which leverages an adaptive entropy loss to mitigate training volatility, ensuring stabilized learning trajectories and enhanced policy robustness compared to the standard PPO.
- Integrating the aforementioned components, extensive experiments demonstrate that TAEPPPO exhibits superior performance on multiple benchmarks.

2 Related Work

2.1 Traditional Methods

Historically, FJSP research has evolved through three paradigms. Initially, exact methods, such as mathematical and constraint programming [Demir and İşleyen, 2013; Yao *et al.*, 2024] solved FJSP by formulating rigorous mixed-integer linear programming (MILP) models. Although these approaches guaranteed optimality through systematic exploration, their exponential complexity renders them impractical for large-scale applications. To mitigate this, metaheuristics were developed, such as evolutionary strategies [Pan *et al.*, 2022; Chen *et al.*, 2025] and swarm optimization [Nouiri *et al.*, 2018; Xu *et al.*, 2024; Shi *et al.*, 2023], employing stochastic search procedures to identify high-quality solutions. However, these methods still struggle with significant overhead in real-time scenarios. Consequently, heuristic priority dispatching rules (PDRs) [Chen and Matis, 2013; Demir and Yilmaz, 2021] are preferred for their efficiency, but often yield suboptimal solutions by relying on simplistic logic such as Most Operations Remaining (MOR) and Most Work Remaining (MWKR) [Sels *et al.*, 2012].

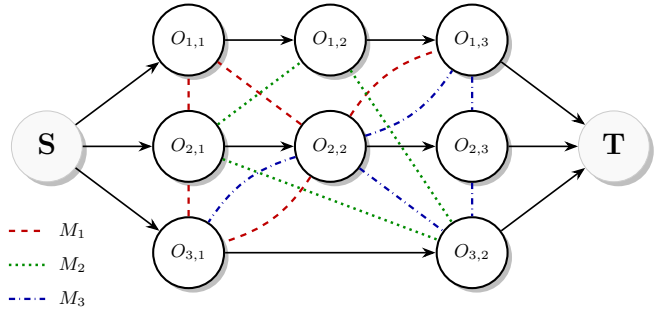


Figure 1: The disjunctive graph of an FJSP instance. The solid arcs represent the precedence constraints within each job, whereas the dashed arcs denote the disjunctive relationships among operations competing for the shared machines.

cant overhead in real-time scenarios. Consequently, heuristic priority dispatching rules (PDRs) [Chen and Matis, 2013; Demir and Yilmaz, 2021] are preferred for their efficiency, but often yield suboptimal solutions by relying on simplistic logic such as Most Operations Remaining (MOR) and Most Work Remaining (MWKR) [Sels *et al.*, 2012].

2.2 DRL-Based Methods

Recently, integrating DRL with GNNs has achieved significant success in addressing FJSP [Zhao *et al.*, 2023; Li *et al.*, 2025; Wu *et al.*, 2025]. The development of effective DRL-based scheduling frameworks has been driven by the introduction of various graph representations, which take advantage of the inherent compatibility of the disjunctive graph [Brandimarte, 1993], employing advanced GNNs to extract rich structural information [Huang *et al.*, 2025; Smit *et al.*, 2025]. In terms of specific methods, heterogeneous GNNs (HGNN) encode intricate relational patterns [Song *et al.*, 2022], while dual attention networks (DANIEL) meticulously capture dynamic shop-floor production features [Wang *et al.*, 2023]. Furthermore, lightweight MLPs (LMDRL) streamline architectures for efficiency [Yuan *et al.*, 2024], while dual operation aggregation GNNs (DOAGNN) model complex dependencies across different jobs [Zhao *et al.*, 2025]. For decision-making, vanilla DRL algorithms, such as standardized proximal policy optimization (PPO) [Schulman *et al.*, 2017] and deep Q-learning (DQN) [Du *et al.*, 2022], are widely applied to facilitate robust optimization of scheduling models. Consequently, developing more sophisticated GNN and refining more robust DRL algorithms constitute a frontier of current investigation.

3 Problem Formulation

The Flexible Job-Shop Scheduling Problem extends the classical Job-Shop Scheduling Problem (JSP) by removing fixed machine constraints. Specifically, it involves n jobs $J = \{J_1, J_2, \dots, J_n\}$ and m machines $M = \{M_1, M_2, \dots, M_m\}$, where each job J_i consists of a sequence of n_i operations $O_i = \{O_{i,1}, O_{i,2}, \dots, O_{i,n_i}\}$ to be processed in order. The set of all operations is denoted by $O = \bigcup_i O_i$. Unlike JSP, each operation $O_{i,j}$ is assignable to any machine in a compatible subset $M_{i,j} \subseteq M$, where the

182 processing time $p_{i,j,k}$ varies depending on the selected ma-
 183 chine M_k . The completion time of $O_{i,j}$ can be denoted as
 184 $C_{i,j}$, and the objective is to minimize the makespan C_{\max}
 185 that represents the completion time of all operations:

$$C_{\max} = \max_{i,j} \{C_{i,j}\}. \quad (1)$$

186 The scheduling of the FJSP is governed by the following sev-
 187 eral constraints:

- **Precedence constraint:** operations within the same job follow a strictly predefined sequence.
- **Assignment constraint:** each operation be allocated to exactly one compatible machine.
- **Exclusivity constraint:** each individual machine can process at most one operation at a time without interruption or preemption.

195 We denote the disjunctive graph $G = (O', C, D)$ for FJSP,
 196 where O' includes all operations and dummy nodes $\{S, E\}$.
 197 Conjunctive arcs C enforce job sequences, while disjunctive
 198 arcs D represent compatible machine assignments. Upon as-
 199 signment of an operation to a specific machine, the corre-
 200 sponding disjunctive arcs in D are transformed into directed
 201 edges, while all conflicting edges are simultaneously eli-
 202 minated to maintain a feasible schedule. Figure 1 illustrates the
 203 disjunctive graph of an FJSP instance.

204 4 Methodology

205 In this section, we present the proposed TAEPPPO in detail.
 206 We formulate FJSP as an Markov Decision Process [Song
 207 *et al.*, 2022; Wang *et al.*, 2023], where decision-making fol-
 208 lows an iterative paradigm. At each step, we select a com-
 209 patible operation-machine pair via the TARAN module that
 210 decouples feature extraction by fusing local operation-level
 211 adjacency and global job-level context relations for opera-
 212 tion embeddings while encoding heterogeneous operation-
 213 machine relations for machine embeddings. These embed-
 214 dings are then concatenated and fed into an actor-critic net-
 215 work refined via the AEPPO algorithm, which incorporates
 216 an adaptive entropy adjustment mechanism to balance explo-
 217 ration and exploitation, ensuring stabilized learning trajec-
 218 tories. The framework of TAEPPPO is illustrated in Figure 2.

219 4.1 Markov Decision Process

220 We formulate the FJSP within a unified MDP framework that
 221 governs the entire scheduling trajectory, from the initial un-
 222 scheduled state to a terminal state. The following sections
 223 present these MDP components, including state representa-
 224 tion, action space, reward mechanism, and state transition.

225 State Representation

226 At each step t , the state of the system s_t consists of op-
 227 erations, machines, and their pair of operations-machines.
 228 For each operation $O_{i,j}$, machine M_k , and compatible pair
 229 $(O_{i,j}, M_k)$, we define their attributes as feature vectors
 230 $h_{O_{i,j}} \in \mathbb{R}^6$, $h_{M_k} \in \mathbb{R}^4$, and $h_{(O_{i,j}, M_k)} \in \mathbb{R}^4$, respectively.
 231 These vectors are engineered to encapsulate critical real-time
 232 status indicators and inherent processing capabilities, thereby
 233 providing the model with a granular and comprehensive view

of the dynamic scheduling environment. Details of these fea-
 234 ture vectors are documented in **Appendix A**.
 235

236 Action Space

237 Let $A(t)$ denote the action space at step t , with $a_t \in A(t)$ rep-
 238 resenting a specific action. To satisfy precedence constraints,
 239 the operation sequencing is restricted to the immediate suc-
 240 cessor of the most recently scheduled one within each job.
 241 Consequently, the candidate operations are upper-bounded by
 242 the job count, yielding a maximum action space cardinality of
 243 $n \times m$ across all machine-assignment permutations.

244 Reward Mechanism

245 The completion time of operation $O_{i,j}$ is defined as its actual
 246 finish time if already scheduled; otherwise, it is iteratively
 247 estimated based on the finish time of its predecessor $O_{i,j-1}$:

$$C(O_{i,j}) = C(O_{i,j-1}) + \frac{\sum_{M_k \in M_{i,j}} p_{i,j,k}}{|M_{i,j}|}, \quad (2)$$

248 where $M_{i,j} \subseteq M$ denotes the set of eligible machines for
 249 $O_{i,j}$. The reward r_t guides the policy towards minimizing
 250 the makespan $C_{\max}(s_t)$, defined as the incremental reduction
 251 in estimated makespan. With a discount factor $\gamma = 1$, the cu-
 252 mulative reward over $T = |O|$ steps is formulated as follows:
 253

$$\begin{aligned} \sum_{t=0}^{T-1} r_t &= \sum_{t=0}^{T-1} [C_{\max}(s_t) - C_{\max}(s_{t+1})] \\ &= C_{\max}(s_0) - C_{\max}(s_T) \xrightarrow{C_{\max}(s_0)=0} -C_{\max}(s_T). \end{aligned} \quad (3)$$

254 Given that $C_{\max}(s_0) = 0$ for an empty initial schedule, the
 255 cumulative reward yields a direct and intrinsic correspon-
 256 dence between the maximization of the reward and the mini-
 257 mization of the final makespan.

258 State Transition

259 Upon taking an action a_t , the environment undergoes a con-
 260 trolled transition from the current state s_t to the subsequent
 261 state s_{t+1} , updating the scheduling configuration and reflect-
 262 ing the real-time allocation of resources within the system.

263 4.2 TARAN Module

264 Specifically, the proposed Topology-Aware Relational At-
 265 tention Networks (TARAN) bifurcates the scheduling graph
 266 learning into dual relational attention streams: one synchro-
 267 nizes local operation-level adjacency with global job-level
 268 context relations to generate enriched operation embeddings,
 269 while the other maps heterogeneous operation-machine rela-
 270 tions into machine embeddings. By integrating these multi-
 271 granular features, TARAN enables a comprehensive state en-
 272 coding that discerns both fine-grained task requirements and
 273 systemic resource constraints.

274 Operation Embeddings

275 Characterizing intricate relations among operations is vital in
 276 FJSP. Local operation-level adjacency delineates precedence
 277 constraints, while global job-level context captures workload
 278 requirements. Integrating these relations enables the model
 279 to bridge sequential logic with global workload distributions,
 which is essential for optimizing scheduling objectives.

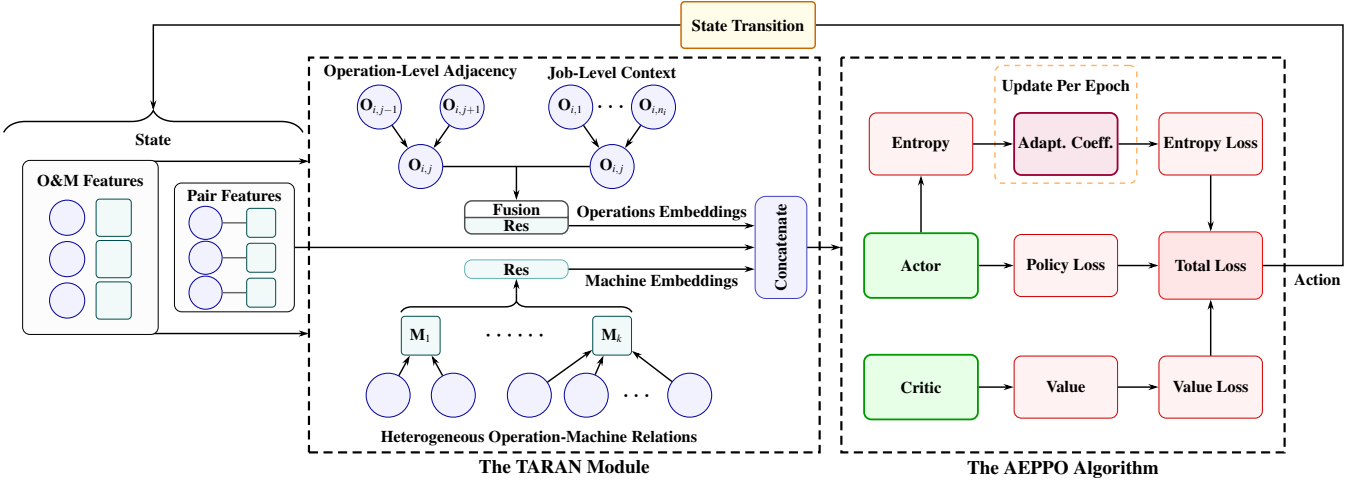


Figure 2: The overall framework of TAEPPo. The TARAN module fuses operation-job features for operation embeddings and encodes operation-machine relations for machine embeddings, while the AEPPO algorithm employs adaptive entropy to stabilize learning trajectories.

For each operation $O_{i,j}$ with raw features $h_{O_{i,j}} \in \mathbb{R}^6$, the attention coefficient between operations $O_{i,j}$ and $O_{i,u}$ in the same job is computed via a shared attention mechanism:

$$e_{i,j,u} = \text{LeakyReLU}(\mathbf{a}_{src}^T \mathbf{W} h_{O_{i,j}} + \mathbf{a}_{dst}^T \mathbf{W} h_{O_{i,u}}), \quad (4)$$

where \mathbf{a}_{src} and $\mathbf{a}_{dst} \in \mathbb{R}^{d_{out}}$ denote the learnable attention vectors, while $\mathbf{W} \in \mathbb{R}^{d_{out} \times 6}$ projects the input features into the latent space. The module bifurcates attention aggregation to capture operation-level adjacency and job-level context:

Operation-Level Adjacency Relations: We denote the attention weight $\alpha_{i,j,u}^{adj}$ to measure the correlation between $O_{i,j}$ and its neighbor $O_{i,u}$. This weight is obtained by normalizing the raw attention coefficients $e_{i,j,u}$:

$$\alpha_{i,j,u}^{adj} = \frac{\exp(e_{i,j,u})}{\sum_{v \in N_{i,j}^{adj}} \exp(e_{i,j,v})}, \quad (5)$$

where $N_{i,j}^{adj} = \{O_{i,j-1}, O_{i,j}, O_{i,j+1}\}$ denotes topologically adjacent operations. The operation-level features for $O_{i,j}$ are synthesized through a weighted aggregation:

$$h_{O_{i,j}}^{adj} = \sum_{u \in N_{i,j}^{adj}} \alpha_{i,j,u}^{adj} \mathbf{W} h_{O_{i,u}}. \quad (6)$$

As initial and terminal operations lack predecessors or successors, we employ an adjacency matrix masking mechanism to filter non-existent dependencies.

Job-Level Context Relations: To capture the context of job J_i , the attention weight $\alpha_{i,j,x}^{job}$ is denoted to quantify the relative importance between $O_{i,j}$ and $O_{i,x}$ within the same job, derived by normalizing the attention coefficients $e_{i,j,x}$:

$$\alpha_{i,j,x}^{job} = \frac{\exp(e_{i,j,x})}{\sum_{y \in N_{i,j}^{job}} \exp(e_{i,j,y})}, \quad (7)$$

where $N_{i,j}^{job}$ denotes all operations belonging to the same job. The aggregated job-level context for $O_{i,j}$ is calculated as:

$$h_{O_{i,j}}^{job} = \sum_{x \in N_{i,j}^{job}} \alpha_{i,j,x}^{job} \mathbf{W} h_{O_{i,x}}. \quad (8)$$

By constructing an intra-job matrix, we can employ a masking mechanism to filter out operations from different jobs.

Channel-Wise Fusion: To balance operation-level adjacency and job-level context, we employ a learnable fusion mechanism. The final embedding $h_{O_{i,j}}^{emb}$ aggregates these representations using channel-wise attention weights and a residual connection to ensure training stability:

$$\begin{aligned} [\lambda_z^{adj}, \lambda_z^{job}] &= \text{Softmax}(\Lambda_z), \\ h_{O_{i,j}}^{emb} &= \lambda_z^{adj} \odot h_{O_{i,j}}^{adj} + \lambda_z^{job} \odot h_{O_{i,j}}^{job} + h_{O_{i,j}}^{res}, \end{aligned} \quad (9)$$

where \odot denotes the element-wise product and $\Lambda \in \mathbb{R}^{d_{out} \times 2}$ is the learnable weight matrix. This fusion enables the model to dynamically prioritize critical features for each operation.

Machine Embeddings

To capture complex operation-machine relations, we propose a heterogeneous networks that maps task-relevant operation features into machine representations. For each machine M_k with raw input h_{M_k} , we denote its neighboring operations as a set N_k . The attention coefficient between M_k and its neighboring operations $O_{i,j} \in N_k$ is defined as follows:

$$e_{i,j,k} = \text{LeakyReLU}(\mathbf{a}_o^T \mathbf{W}_o h_{O_{i,j}} + \mathbf{a}_m^T \mathbf{W}_m h_{M_k}), \quad (10)$$

where \mathbf{W}_o and \mathbf{W}_m represent learnable weight matrices that project features into a shared latent space, while \mathbf{a}_o and \mathbf{a}_m denote the corresponding weight vectors for operations and machines, respectively.

Operation-Machine Relations: Similarly, these coefficients are then normalized via a softmax function across all neighboring operations:

$$\alpha_{i,j,k} = \frac{\exp(e_{i,j,k})}{\sum_{O_{u,v} \in N_k} \exp(e_{u,v,k})}. \quad (11)$$

By incorporating a residual connection, the final embedding of machine M_k is obtained as follows:

$$h_{M_k}^{emb} = \sum_{O_{i,j} \in N_k} \alpha_{i,j,k} \mathbf{W}_o h_{O_{i,j}} + h_{M_k}^{res}. \quad (12)$$

329 Through this formulation, the model effectively encapsulates
 330 the operation-machine relations, enabling the machine em-
 331 beddings to assimilate heterogeneous structural information.

332 State Embeddings

333 The state embedding is synthesized by performing and
 334 concatenating average pooling over both operation embeddings
 335 and machine embeddings as follows:

$$h_{st} = \left[\frac{1}{|O|} \sum_{O_{i,j} \in O} h_{O_{i,j}}^{emb} \middle\| \frac{1}{|M|} \sum_{M_k \in M} h_{M_k}^{emb} \right]. \quad (13)$$

336 This state embedding integrates operation-level and machine-
 337 level features, delivering a comprehensive overview of the
 338 global state for each decision-making step.

339 4.3 AEPPO Algorithm

340 To solve FJSP, we employ Adaptive-Entropy Proximal Pol-
 341 icy Optimization (AEPPO), enhanced with a dynamic entropy
 342 regularization mechanism. This ensures a robust balance be-
 343 tween exploration and exploitation in the high-dimensional
 344 discrete action space of scheduling. Diverging from standard
 345 PPO, AEPPO utilizes stochastic mini-batch sampling from
 346 collected trajectories to stabilize gradient updates and im-
 347 prove data efficiency. The algorithmic procedure is detailed
 348 in Algorithm 1.

349 Actor-Critic

350 The policy and value functions are implemented through an
 351 actor-critic architecture, where two distinct multilayer per-
 352 ceptrons (MLPs) serve as the actor π_θ and the critic v_ϕ , re-
 353 spectively. For each action $a_t = (O_{ij}, M_k) \in A_t$, the actor
 354 computes priority index $P(a_t|s_t)$ by processing concatenated
 355 operation, machine embeddings, and pair features, and the ac-
 356 tion selection probability $\pi_\theta(a_t|s_t)$ is normalized over $A(t)$:

$$\begin{aligned} P(a_t|s_t) &= \text{MLP}_\theta \left[h_{O_{i,j}}^{emb} \| h_{M_k}^{emb} \| h_{(O_{i,j}, M_k)} \right], \\ \pi_\theta(a_t|s_t) &= \frac{\exp(P(a_t|s_t))}{\sum_{a'_t \in A(t)} \exp(P(a'_t|s_t))}. \end{aligned} \quad (14)$$

357 Furthermore, the critic estimates the state value $v_\phi(s_t)$ us-
 358 ing the state embedding:

$$v_\phi(s_t) = \text{MLP}_\phi(h_{st}). \quad (15)$$

359 Policy and Value Loss

360 To ensure stable updates, the PPO-clip objective employs the
 361 ratio $r_t(\theta) = \pi_\theta(a_t|s_t)/\pi_{\theta_{old}}(a_t|s_t)$ that denotes the prob-
 362 ability ratio between current and old behavioral policies to
 363 penalize policy deviations outside the $[1 - \epsilon, 1 + \epsilon]$ interval:

$$\begin{aligned} \mathcal{L}^{POL} &= C_p \cdot \{-\mathbb{E}_t[\min(r_t(\theta)\hat{A}_t, \\ &\text{clip}(r_t(\theta), 1 - \epsilon, 1 + \epsilon)\hat{A}_t)]\}, \end{aligned} \quad (16)$$

364 where ϵ is the clipping hyperparameter, \hat{A}_t is the advantage
 365 estimation, and C_p is the policy loss coefficient.

366 The value loss is the Mean Squared Error (MSE) between
 367 the predicted value and discounted rewards R_t :

$$\mathcal{L}^{VAL} = C_v \cdot \mathbb{E}_t \left[(v_\phi(s_t) - R_t)^2 \right], \quad (17)$$

368 where C_v denotes the value loss coefficient and $v_\phi(s_t)$ repre-
 369 sents the estimated state value.

Algorithm 1 The training process of AEPPO

Input: Pre-sampled training data D_{tra} , validation data D_{val}
Parameter: Initial policy parameters π_θ , value parameters
 v_ϕ , entropy coefficient parameters C_e
Output: The trained optimal π_θ

- 1: **for** iteration = 1, 2, ..., T **do**
- 2: Collect trajectories $\mathcal{T} = \{s_t, a_t, r_t, s_{t+1}\}$ of D_{tra} .
- 3: Estimate target entropy H_{tar} using Eq. (18), compute
 estimated advantages \hat{A}_t and discounted rewards R_t .
- 4: **for** epoch = 1, ..., K **do**
- 5: **for** each minibatch $B_{min} \sim D_{tra}$ **do**
- 6: Calculate losses $\{\mathcal{L}^{POL}, \mathcal{L}^{VAL}, \mathcal{L}^{ENT}\}$ accord-
 ing to Eqs. (16), (17), and (20).
- 7: Calculate total loss \mathcal{L}^{TOT} using Eq. (21).
- 8: Update parameters π_θ, v_ϕ .
- 9: **end for**
- 10: Update entropy coefficient C_e using Eq. (19).
- 11: **end for**
- 12: Resample $|D_{tra}|$ FJSP instances every T_{tra} iteration.
- 13: Validate π_θ on D_{val} every T_{val} iteration.
- 14: **end for**
- 15: **return** Optimal π_θ

Adaptive Entropy Loss

In FJSP, the feasible action space cardinality varies across
 371 decision-making stages. We implement an automated tuning
 372 loop for entropy coefficient C_e , defining target entropy H_{tar}
 373 based on the average number of eligible actions A_e :

$$A_e = \sum_{a_t \in A(t)} m(a_t|s_t), \quad (18)$$

$$H_{tar} = \beta \cdot \ln(A_e + 10^{-8}),$$

where $m(a_t|s_t) \in \{0, 1\}$ is a binary indicator that denotes
 375 the feasibility of action a_t in state and β is a conservative em-
 376 pirical target density. While the policy updates for K epochs
 377 per iteration, $\log C_e$ is optimized epoch-wise by minimizing:
 378

$$\mathcal{L}(C_e) = \log C_e \cdot (H_{avg} - H_{tar}), \quad (19)$$

where H_{avg} is the mean entropy observed during the epoch.
 379 This mechanism ensures that C_e increases when the policy
 380 becomes overly deterministic and decreases once the target
 381 exploration level is reached. The entropy loss is denoted as:
 382

$$\mathcal{L}^{ENT} = -C_e \cdot \hat{\mathbb{E}}_t [H_s(\pi_\theta(\cdot|s_t))], \quad (20)$$

where H_s denotes the Shannon entropy of the action distribu-
 383 tion. Our AEPPO diverges from Soft Actor-Critic [Haarnoja
 384 et al., 2018] by employing a dynamic entropy target tailored
 385 to varying action spaces with specialized update formulation.
 386 Theoretical justification is provided in **Appendix B**.
 387

Total Loss

Combining the policy loss, the value loss, and the adaptive
 388 entropy loss, the total loss is defined as follows:
 389

$$\mathcal{L}^{TOT} = \mathcal{L}^{POL} + \mathcal{L}^{VAL} + \mathcal{L}^{ENT}. \quad (21)$$

In summary, this composite loss function empowers TAEPPPO
 390 with enhanced numerical stability and robust convergence,
 392 ensuring reliable performance when navigating the complex
 393 combinatorial decision-making space of FJSP environments.
 394

Methods	Brandimarte		Rdata		Edata		Vdata		
	$C_{max} \downarrow$	Gap \downarrow							
Traditional PDRs	FIFO	205.56	31.82%	1087.12	17.25%	1244.92	20.83%	982.89	7.58%
	SPT	237.52	44.88%	1200.41	29.47%	1312.84	26.79%	1082.88	18.20%
	MOR	200.36	28.08%	1066.73	15.07%	1227.07	19.24%	966.01	5.68%
	MWKR	201.74	28.91%	1053.10	13.86%	1219.01	18.60%	952.00	4.22%
HGNN	10×5	201.00	27.83%	1030.83	11.15%	1187.47	15.53%	955.90	4.25%
	15×10	197.70	25.39%	1031.33	11.14%	1182.08	15.00%	954.33	4.02%
DANIEL	10×5	185.70	13.58%	1031.63	11.42%	1194.98	16.33%	944.85	3.28%
	15×10	184.40	12.97%	1040.05	12.07%	1175.53	14.41%	948.73	3.75%
LMDRL DOAGNN	10×5	186.80	13.24%	1041.83	12.09%	1187.93	15.54%	963.50	5.37%
	10×5	199.60	30.43%	1040.45	12.05%	1189.40	15.67%	958.80	4.73%
TAEPPPO (ours)	10×5	187.10	14.73%	1017.60	9.43%	1169.78	13.76%	947.03	3.26%
	15×10	183.00	11.71%	1023.25	10.27%	1179.78	14.65%	943.43	3.14%

Table 1: Overall performance of our TAEPPPO and baselines on four benchmarks. Bold indicates the best performance.

395 5 Experiments

396 5.1 Experimental Setup

397 Datasets

398 We conduct our experiments on four public benchmarks comprising various FJSP instances [Behnke and Geiger, 2012]:
400 Brandimarte dataset (Mk01-10) [Brandimarte, 1993] and
401 three sets of Hurink datasets (Rdata, Edata, and Vdata, each
402 set consists of La01-40) [Hurink *et al.*, 1994], consistent
403 with previous studies [Song *et al.*, 2022; Wang *et al.*, 2023;
404 Yuan *et al.*, 2024; Zhao *et al.*, 2025]. Specifically, models
405 are trained on two problem sizes: 10×5 and 15×10 , where
406 training instances are generated following [Song *et al.*, 2022].
407 Subsequently, the optimal trained policy is saved and evaluated
408 on benchmarks to assess the performance of TAEPPPO on
409 out-of-distribution instances.

410 Baselines

411 Initially, we evaluate our proposed approach against four
412 standard heuristic PDRs, including FIFO (First In First Out),
413 SPT (Shortest Processing Time), MOR (Most Operations Re-
414 maining), and MWKR (Most Work Remaining). Furthermore,
415 our comparative analysis focuses on four state-of-the-art DRL-based
416 methodologies: HGNN [Song *et al.*, 2022], DANIEL [Wang *et al.*, 2023], LMDRL [Yuan *et al.*, 2024],
417 and DOAGNN [Zhao *et al.*, 2025]. As elaborated in the
418 Related Work section, these methods leverage sophisticated
419 graph representations and various GNNs to address intricate
420 scheduling challenges.

422 Evaluation Metrics

423 In addition to the makespan metric C_{max} , we also employ
424 the average relative gap to comprehensively evaluate per-
425 formance. This metric quantifies the deviation between the
426 achieved C_{max} and the best-known solutions C_{max}^{best} reported
427 in [Behnke and Geiger, 2012], defined as:

$$428 \text{Gap} = \left(\frac{C_{max}}{C_{max}^{best}} - 1 \right) \times 100\%. \quad (22)$$

Implementation Details

The total number of training iterations, parallel batch size, and validation interval are set to 1000, 20, and 10, respectively. The PPO algorithm utilizes the AdamW optimizer with a learning rate of 3×10^{-4} . For testing, we exclusively evaluate and compare results using a greedy decoding strategy for all benchmarks. All experiments were conducted on a server equipped with an Intel Xeon Silver 4310 CPU and an NVIDIA GeForce RTX 4090 GPU. More details can be found in Appendix C. Our source code is available in the Supplementary Material.

5.2 Results and Analysis

Table 1 presents the comparative performance of TAEPPPO compared to traditional PDRs and DRL-based baselines on the benchmark datasets. In general, TAEPPPO achieves state-of-the-art results, outperforming all baselines in terms of both makespan and relative gap and demonstrating its exceptional capability in handling complex scheduling scenarios.

Compared to traditional PDRs, our method exhibits a markedly superior performance margin. In particular, it reduces the relative gap by more than 15% on the Brandimarte dataset and by more than 4% on both Rdata and Edata benchmarks, relative to the most competitive PDRs. These empirical results underscore the intrinsic limitations of heuristic PDRs in navigating the high-dimensional solution space of FJSP environments. In contrast, TAEPPPO successfully derives dynamic and precise dispatching rules tailored to sophisticated topological relations.

Furthermore, TAEPPPO outperforms DRL baselines with a substantial and measurable reduction in both the average makespan and the relative gap. Specifically, the TAEPPPO model trained on 10×5 scale achieves an average makespan of 1017.60 and a mean gap of 9.43% on the Rdata benchmark, while all baseline models exceed 1030 and 11%, respectively. Similarly, on the Brandimarte dataset, the 15×10 model yields solutions with a makespan of 183.00 and a gap of 11.71%, surpassing the best-performing baselines. We at-

Components		Brandimarte		Rdata		Edata		Vdata	
TARAN	AEPPO	$C_{max} \downarrow$	Gap \downarrow						
✗	✗	191.10	15.97%	1049.65	12.94%	1195.73	16.47%	971.15	5.86%
✓	✗	185.60	13.73%	1039.58	11.80%	1191.73	16.03%	961.65	5.06%
✗	✓	188.70	14.99%	1044.90	12.18%	1198.60	16.65%	985.38	7.55%
✓	✓	183.00	11.71%	1023.25	10.27%	1179.78	14.65%	943.43	3.14%

Table 2: Ablation study of two core components of TAEPPo on public benchmarks.

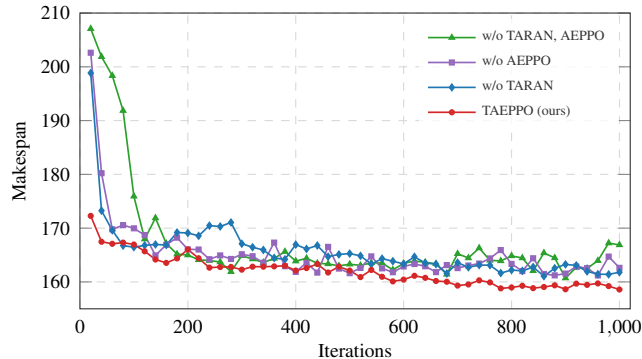


Figure 3: Training curves for the ablation study. Both TARAN and AEPPO modules significantly accelerate convergence while achieving optimal performance.

tribute this significant performance gain to the respective contributions of the proposed TARAN module and AEPPO algorithm. The former utilizes three topological relations to facilitate precise state encoding, while the latter enables the agent to converge to high-quality solutions with enhanced robustness via an adaptive entropy adjustment mechanism.

5.3 Ablation Study

Ablation studies are performed by substituting TARAN with parameter-equivalent MLPs and replacing AEPPO with vanilla PPO using a constant entropy coefficient to isolate their respective contributions. All variants are trained on 15×10 instances and evaluated on all benchmarks to quantify their relative and empirical effectiveness.

As illustrated by the training curves in Figure 3, variants lacking TARAN or AEPPO suffer from compromised optimization stability and inferior convergence rates, directly correlating with the observed degradation in generalization capability and final validation performance. Table 2 presents the ablation results of TAEPPo on public benchmarks. Without the TARAN module, the model fails to capture the intrinsic topological relations of the disjunctive graph, which limits its ability to encode comprehensive state representations. Similarly, in the absence of the AEPPO algorithm, the agent with fixed-entropy PPO struggles to manage exploration-exploitation trade-offs across varying problem scales, resulting in a significant drop in solution quality. Ultimately, the ablation study confirms that both TARAN and AEPPO are indispensable components, each contributing uniquely to the superior performance of TAEPPo.

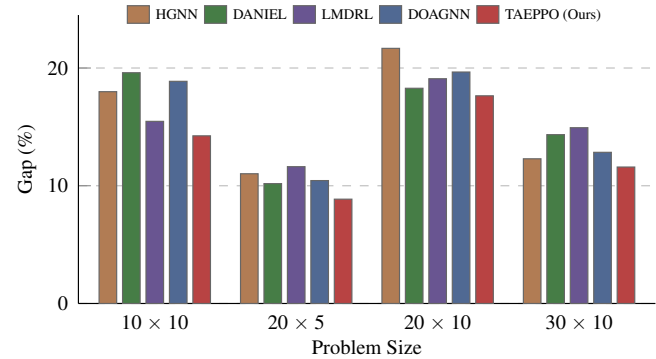


Figure 4: Generalization performance of TAEPPo compared to DRL-based baselines across unseen problem scales.

5.4 Generalization Capability

A generalization experiment is conducted to rigorously evaluate the zero-shot performance of DRL-based methods trained on 10×5 instances when applied to out-of-distribution (OOD) problem scales. We report the average gap calculated across five independent instances for each problem scale within the Edata benchmark. As illustrated in Figure 4, TAEPPo consistently outperforms all baselines in four OOD scenarios. Consequently, the 10×5 TAEPPo model maintains its advantage in larger 20×10 and 30×10 cases, underscoring its superior generalization and robustness to unseen scales. This suggests TAEPPo captures scale-invariant topological relations rather than merely overfitting to the training distribution.

6 Conclusion

In this paper, we present TAEPPo, a novel DRL-based framework designed to tackle the inherent complexities of FJSP. The TAEPPo framework synergistically integrates TARAN and AEPPO, facilitating effective and adaptive scheduling by leveraging enhanced topological awareness and stabilized policy updates. Specifically, TARAN employs dual relations attention networks to capture the intricate structural relations between operations and machines, while AEPPO incorporates an automated entropy regularization scheme to dynamically balance exploration and exploitation throughout the solution space search. Experimental results across various benchmarks demonstrate that TAEPPo not only significantly outperforms both traditional PDRs and state-of-the-art DRL-based methods but also exhibits superior generalization capability when applied to unseen problem scales.

References

- [Ahmed *et al.*, 2022] Imran Ahmed, Gwanggil Jeon, and Francesco Piccialli. From artificial intelligence to explainable artificial intelligence in industry 4.0: a survey on what, how, and where. *IEEE transactions on industrial informatics*, 18(8):5031–5042, 2022.
- [Ahsan and Siddique, 2022] Md Manjurul Ahsan and Zahed Siddique. Industry 4.0 in healthcare: A systematic review. *International Journal of Information Management Data Insights*, 2(1):100079, 2022.
- [Behnke and Geiger, 2012] Dennis Behnke and Martin Josef Geiger. Test instances for the flexible job shop scheduling problem with work centers. *Arbeitspapier / research report*, HELMUT-SCHMIDT-UNIVERSITÄT, 2012.
- [Brandimarte, 1993] Paolo Brandimarte. Routing and scheduling in a flexible job shop by tabu search. *Annals of Operations research*, 41(3):157–183, 1993.
- [Chaudhry and Khan, 2016] Imran Ali Chaudhry and Abid Ali Khan. A research survey: review of flexible job shop scheduling techniques. *International Transactions in Operational Research*, 23(3):551–591, 2016.
- [Chen and Matis, 2013] Binchao Chen and Timothy I Matis. A flexible dispatching rule for minimizing tardiness in job shop scheduling. *International Journal of Production Economics*, 141(1):360–365, 2013.
- [Chen *et al.*, 2025] Xiaolong Chen, Junqing Li, Zunxun Wang, Qingda Chen, Kaizhou Gao, and Quanke Pan. Optimizing dynamic flexible job shop scheduling using an evolutionary multi-task optimization framework and genetic programming. *IEEE Transactions on Evolutionary Computation*, 2025.
- [Corso *et al.*, 2024] Gabriele Corso, Hannes Stark, Stefanie Jegelka, Tommi Jaakkola, and Regina Barzilay. Graph neural networks. *Nature Reviews Methods Primers*, 4(1):17, 2024.
- [Dauzère-Pérès *et al.*, 2024] Stéphane Dauzère-Pérès, Junwen Ding, Liji Shen, and Karim Tamssouet. The flexible job shop scheduling problem: A review. *European Journal of Operational Research*, 314(2):409–432, 2024.
- [Demir and İşleyen, 2013] Yunus Demir and S Kürşat İşleyen. Evaluation of mathematical models for flexible job-shop scheduling problems. *Applied Mathematical Modelling*, 37(3):977–988, 2013.
- [Demir and Yilmaz, 2021] Yunus Demir and Hamid Yilmaz. An efficient priority rule for flexible job shop scheduling problem. *Journal of Engineering Research and Applied Science*, 10(2):1906–1918, 2021.
- [Du *et al.*, 2022] Yu Du, Junqing Li, Chengdong Li, and Peiyong Duan. A reinforcement learning approach for flexible job shop scheduling problem with crane transportation and setup times. *IEEE Transactions on Neural Networks and Learning Systems*, 35(4):5695–5709, 2022.
- [Gao *et al.*, 2019] Kaizhou Gao, Zhiguang Cao, Le Zhang, Zhenghua Chen, Yuyan Han, and Quanke Pan. A review on swarm intelligence and evolutionary algorithms for solving flexible job shop scheduling problems. *IEEE/CAA Journal of Automatica Sinica*, 6(4):904–916, 2019.
- [Haarnoja *et al.*, 2018] Tuomas Haarnoja, Aurick Zhou, Pieter Abbeel, and Sergey Levine. Soft actor-critic: Off-policy maximum entropy deep reinforcement learning with a stochastic actor. In *International conference on machine learning*, pages 1861–1870. Pmlr, 2018.
- [Han and Yang, 2021] Baoan Han and J Yang. A deep reinforcement learning based solution for flexible job shop scheduling problem. *International Journal of Simulation Modelling*, 20(2):375–386, 2021.
- [Huang *et al.*, 2025] Dailin Huang, Hong Zhao, Weiquan Tian, and Kangping Chen. A deep reinforcement learning method based on a multiexpert graph neural network for flexible job shop scheduling. *Computers & Industrial Engineering*, 200:110768, 2025.
- [Hurink *et al.*, 1994] Johann Hurink, Bernd Jurisch, and Monika Thole. Tabu search for the job-shop scheduling problem with multi-purpose machines. *Operations-Research-Spektrum*, 15(4):205–215, 1994.
- [Lei *et al.*, 2022] Kun Lei, Peng Guo, Wenchao Zhao, Yi Wang, Linmao Qian, Xiangyin Meng, and Liansheng Tang. A multi-action deep reinforcement learning framework for flexible job-shop scheduling problem. *Expert Systems with Applications*, 205:117796, 2022.
- [Lei *et al.*, 2023] Kun Lei, Peng Guo, Yi Wang, Jian Zhang, Xiangyin Meng, and Linmao Qian. Large-scale dynamic scheduling for flexible job-shop with random arrivals of new jobs by hierarchical reinforcement learning. *IEEE Transactions on Industrial Informatics*, 20(1):1007–1018, 2023.
- [Li *et al.*, 2025] Yuxin Li, Qingzheng Wang, Xinyu Li, Liang Gao, Ling Fu, Yanbin Yu, and Wei Zhou. Real-time scheduling for flexible job shop with agvs using multiagent reinforcement learning and efficient action decoding. *IEEE Transactions on Systems, Man, and Cybernetics: Systems*, 2025.
- [Liu *et al.*, 2022] Renke Liu, Rajesh Piplani, and Carlos Toro. Deep reinforcement learning for dynamic scheduling of a flexible job shop. *International Journal of Production Research*, 60(13):4049–4069, 2022.
- [Mahmoodi *et al.*, 2024] Ehsan Mahmoodi, Masood Fathi, Majid Tavana, Morteza Ghobakhloo, and Amos HC Ng. Data-driven simulation-based decision support system for resource allocation in industry 4.0 and smart manufacturing. *Journal of Manufacturing Systems*, 72:287–307, 2024.
- [Meng *et al.*, 2020] Leilei Meng, Chaoyong Zhang, Yaping Ren, Biao Zhang, and Chang Lv. Mixed-integer linear programming and constraint programming formulations for solving distributed flexible job shop scheduling problem. *Computers & industrial engineering*, 142:106347, 2020.
- [Nouiri *et al.*, 2018] Maroua Nouiri, Abdelghani Bekrar, Abderezak Jemai, Smail Niar, and Ahmed Chiheb Am-

- 632 mari. An effective and distributed particle swarm opti-
 633 mization algorithm for flexible job-shop scheduling prob-
 634 lem. *Journal of Intelligent Manufacturing*, 29(3):603–615,
 635 2018.
- 636 [Pan *et al.*, 2022] Zixiao Pan, Ling Wang, Jie Zheng, Jing-
 637 Fang Chen, and Xing Wang. A learning-based multi-
 638 population evolutionary optimization for flexible job
 639 shop scheduling problem with finite transportation re-
 640 sources. *IEEE Transactions on Evolutionary Compu-
 641 tation*, 27(6):1590–1603, 2022.
- 642 [Schulman *et al.*, 2017] John Schulman, Filip Wolski, Pra-
 643 fulla Dhariwal, Alec Radford, and Oleg Klimov. Prox-
 644 imal policy optimization algorithms. *arXiv preprint
 645 arXiv:1707.06347*, 2017.
- 646 [Sels *et al.*, 2012] Veronique Sels, Nele Gheysen, and Mario
 647 Vanhoucke. A comparison of priority rules for the job
 648 shop scheduling problem under different flow time-and
 649 tardiness-related objective functions. *International Jour-
 650 nal of Production Research*, 50(15):4255–4270, 2012.
- 651 [Shi *et al.*, 2023] Jiaxuan Shi, Mingzhou Chen, Yumin Ma,
 652 and Fei Qiao. A new boredom-aware dual-resource con-
 653 strained flexible job shop scheduling problem using a two-
 654 stage multi-objective particle swarm optimization algo-
 655 rithm. *Information Sciences*, 643:119141, 2023.
- 656 [Smit *et al.*, 2025] Igor G Smit, Jianan Zhou, Robbert Rei-
 657 jnen, Yaoxin Wu, Jian Chen, Cong Zhang, Zaharah
 658 Bukhsh, Yingqian Zhang, and Wim Nuijten. Graph neu-
 659 ral networks for job shop scheduling problems: A survey.
 660 *Computers & Operations Research*, 176:106914, 2025.
- 661 [Song *et al.*, 2022] Wen Song, Xinyang Chen, Qiqiang Li,
 662 and Zhiguang Cao. Flexible job-shop scheduling via graph
 663 neural network and deep reinforcement learning. *IEEE
 664 Transactions on Industrial Informatics*, 19(2):1600–1610,
 665 2022.
- 666 [Wang *et al.*, 2021] Libing Wang, Xin Hu, Yin Wang, Sujei
 667 Xu, Shijun Ma, Kexin Yang, Zhijun Liu, and Weidong
 668 Wang. Dynamic job-shop scheduling in smart manufac-
 669 turing using deep reinforcement learning. *Computer net-
 670 works*, 190:107969, 2021.
- 671 [Wang *et al.*, 2023] Runqing Wang, Gang Wang, Jian Sun,
 672 Fang Deng, and Jie Chen. Flexible job shop scheduling
 673 via dual attention network-based reinforcement learning.
 674 *IEEE Transactions on Neural Networks and Learning Sys-
 675 tems*, 35(3):3091–3102, 2023.
- 676 [Wang *et al.*, 2025] Zunxun Wang, Junqing Li, Xiaolong
 677 Chen, Peiyong Duan, and Jiake Li. Uncertain inter-
 678 ruptibility multiobjective flexible job shop via deep re-
 679inforcement learning based on heterogeneous graph self-
 680 attention. *IEEE Transactions on Neural Networks and
 681 Learning Systems*, 2025.
- 682 [Wu *et al.*, 2025] Lincong Wu, Xiaoxia Li, Xin Lu, Zaiwen
 683 Feng, and Yanguo Jing. An adaptive meta-reinforcement
 684 learning framework for dynamic flexible job shop schedul-
 685 ing. *IEEE Transactions on Automation Science and Engi-
 686 neering*, 22:24036–24052, 2025.
- 687 [Xie *et al.*, 2019] Jin Xie, Liang Gao, Kunkun Peng, Xinyu
 688 Li, and Haoran Li. Review on flexible job shop scheduling.
 689 *IET collaborative intelligent manufacturing*, 1(3):67–77,
 690 2019.
- 691 [Xu *et al.*, 2021] Xun Xu, Yuqian Lu, Birgit Vogel-Heuser,
 692 and Lihui Wang. Industry 4.0 and industry 5.0—incep-
 693 tion, conception and perception. *Journal of manufacturing
 694 systems*, 61:530–535, 2021.
- 695 [Xu *et al.*, 2024] Yuanxing Xu, Mengjian Zhang, Ming
 696 Yang, and Deguang Wang. Hybrid quantum particle
 697 swarm optimization and variable neighborhood search for
 698 flexible job-shop scheduling problem. *Journal of Manu-
 699 facturing Systems*, 73:334–348, 2024.
- 700 [Yao *et al.*, 2024] Youjie Yao, Qihao Liu, Ling Fu, Xinyu Li,
 701 Yanbin Yu, Liang Gao, and Wei Zhou. A novel mathemat-
 702 ical model for the flexible job-shop scheduling problem
 703 with limited automated guided vehicles. *IEEE Transac-
 704 tions on Automation Science and Engineering*, 2024.
- 705 [Yuan *et al.*, 2024] Erdong Yuan, Liejun Wang, Shuli Cheng,
 706 Shiji Song, Wei Fan, and Yongming Li. Solving flexi-
 707 ble job shop scheduling problems via deep reinforcement
 708 learning. *Expert Systems with Applications*, 245:123019,
 709 2024.
- 710 [Zhang *et al.*, 2024] Wenquan Zhang, Fei Zhao, Yong Li,
 711 Chao Du, Xiaobing Feng, and Xuesong Mei. A novel col-
 712 laborative agent reinforcement learning framework based
 713 on an attention mechanism and disjunctive graph embed-
 714 ding for flexible job shop scheduling problem. *Journal of
 715 Manufacturing Systems*, 74:329–345, 2024.
- 716 [Zhao *et al.*, 2023] Linlin Zhao, Jiaxin Fan, Chunjiang
 717 Zhang, Weiming Shen, and Jing Zhuang. A drl-based reac-
 718 tive scheduling policy for flexible job shops with random
 719 job arrivals. *IEEE Transactions on Automation Science
 720 and Engineering*, 21(3):2912–2923, 2023.
- 721 [Zhao *et al.*, 2025] Peng Zhao, You Zhou, Di Wang,
 722 Zhiguang Cao, Yubin Xiao, Xuan Wu, Yuanshu Li,
 723 Hongjia Liu, Wei Du, Yuan Jiang, et al. Dual operation
 724 aggregation graph neural networks for solving flexible job-
 725 shop scheduling problem with reinforcement learning. In
 726 *Proceedings of the ACM on Web Conference 2025*, pages
 727 4089–4100, 2025.
- 728 [Zhou *et al.*, 2020] Jie Zhou, Ganqu Cui, Shengding Hu,
 729 Zhengyan Zhang, Cheng Yang, Zhiyuan Liu, Lifeng
 730 Wang, Changcheng Li, and Maosong Sun. Graph neural
 731 networks: A review of methods and applications. *AI open*,
 732 1:57–81, 2020.